ARID ZONE JOURNAL OF ENGINEERING, TECHNOLOGY & ENVIRONMENT
AZOJETE September 2024. Vol. 20(4):699-712
Published by the Faculty of Engineering, University of Maiduguri, Maiduguri, Nigeria.
Print ISSN: 1596-2490, Electronic ISSN: 2545-5818
www.azojete.com.ng

ANALYSIS OF NORMAL RADAR SIGNAL BASED ON DIFFERENT TIME-FREQUENCY DISTRIBUTION CONFIGURATIONS

A. A. Ahmad[1]*, M. M. Aji[1], M. Abdulkadir[2], F. O. Adunola[1] and S. Lawan[1]

[1]Department of Electrical and Electronic Engineering, Nigerian Defence Academy, Kaduna
[2]Department of Electrical and Electronic Engineering, University of Maiduguri, Maiduguri, Borno State
**Corresponding author's email address: aaashraf@nda.edu.ng*

ARTICLE INFORMATION

Submitted 11 July, 2023
Revised 27 June, 2024
Accepted 10 July, 2024

Keywords:
Radar Signal
Time-Frequency Distribution
Electronic Intelligence (ELINT)
Waterfall Plot
Hilbert Transform
Frequency Agility
Electronic Warfare Support (ES)

ABSTRACT

The electromagnetic environment is becoming more complex, and radar technology is always evolving, as such, a sizable number of contemporary radars with agile waveforms have appeared on the battlefield. Relying solely on traditional recognition models to identify radar signals in electronic warfare systems is a significant challenge. In response to the this problem, this paper proposed an analysis of normal radar signal based on different time-frequency distribution (TFDs) configurations which include Wigner-Ville Distribution (WVD), Windowed Wille-Ville Distribution (WWVD), Filtered Wigner-Ville Distribution (FWVD), Choi Williams Distribution (CWD), and hybrid distributions that combined FWVD and CWD.A two-stage process in other to achieve the aim of this research is presented. The first stage is the modelling and generating a normal (simple) radar signal of pulse-to-pulse constant frequency, while the second stage involved designed of these TFDs and using them to analyse the radar signals. The result showed that most of the TFDs captured the time and frequency parameters of the radar signals modelled around of pulse width (PW) of 1µs, pulse repetition interval (PRI) of 2 µs, center and sampling frequencies of 10 MHz and 40 MHz respectively. Therefore, these TFDs can further be analysed using signal processing and classification tools such as instantaneous power, instantaneous frequency, and machine learning for automatic waveform recognition.

1.0 Introduction

Radar, which stands for Radio Detection and Ranging, is a technology that uses radio waves to detect and track objects in various applications (Patole *et al.*, 2017). The versatility and reliability of radar make it an essential tool in numerous fields. To explore some of these normal application areas of radar includes crucial role in aviation for air traffic control, collision avoidance, and weather monitoring, in military and defense applications. It is also utilized for air defense, surveillance, target tracking, and missile guidance. In maritime navigation, radar systems are used for collision avoidance, safe passage planning, and vessel traffic management. Additionally, radar is employed to monitor and track precipitation, storms, and severe weather phenomena. Fourier analysis techniques, including the Fast Fourier Transform (FFT), are applied in digital intercept receivers to detect and analyze parameters of low probability of intercept (LPI) radar signals (Pace, 2009).

When a practical non-stationary signal (such as a noised normal radar signal) is processed, the Fourier transform cannot efficiently analyze and process the time-varying characteristics of the signal's frequency spectrum, because time and frequency information cannot be combined to tell how the frequency content is changing in time (Stephens, 1996; Xie *et al.*, 2008). The non-stationary nature of the received radar signal mandates the use of some form of time-frequency analysis for signal detection and parameter extraction (Ünal and Pakfiliz, 2022). Some of the more common classical time-frequency analysis techniques include the WVD, CWD, spectrogram, and scalogram. The WVD exhibits the highest signal energy concentration (Wiley, 2006). but has the worse cross-term interference, which can severely limit the readability of a time-frequency representation (Stephens, 1996; Gulum, 2007; Boashash, 2015). The CWD is a member of Cohen's class, which adds a smoothing kernel to help reduce cross-term interference (Upperman, 2008; Boashash, 2015). The CWD, as with all members of Cohen's class, is faced with a trade-off between cross-term reduction and time-frequency localization.

Radar waveforms are susceptible to various forms of noise and interference, including thermal noise, clutter, and jamming signals (Wei *et al.*, 2014). The presence of unwanted components such as noise and interference in radar signals can significantly deteriorate the quality of time-frequency representation, leading to inaccurate radar parameter estimation. Therefore, it is crucial to develop robust time-frequency analysis techniques that effectively mitigate the effects of these unwanted components. Additionally, radar waveforms often exhibit nonstationary and transient behavior due to various factors such as target dynamics, modulation schemes, or environmental conditions. Time-frequency distributions (TFDs) employed for radar waveform analysis should be capable of capturing the non-stationary nature of signals and accurately representing transient features. Techniques that adapt to signal variations over time or provide localized time-frequency analysis are necessary to address these nonstationary aspects. Furthermore, in real-time radar applications, efficient algorithms and techniques for time-frequency analysis are required. The computational complexity of time-frequency distributions should be manageable to facilitate their implementation in resource-constrained radar systems. Hence, it is essential to develop computationally efficient methods that strike a balance between accuracy and computational requirements, as this is crucial for practical radar waveform analysis. Addressing these challenges through the utilization of TFDs contributes to the advancement of radar system capabilities, ultimately enhancing target detection, classification, and tracking performance. The research presented in this paper focuses on the careful design and adoption of commonly used TFDs to effectively tackle these challenges (Boashash, 2015; Ahmad *et al.*, 2019).

Radar waveforms face various noise and interference issues, such as thermal noise, clutter, and jamming signals (Wei *et al.*, 2014). These unwanted components can degrade time-frequency representations and lead to inaccurate parameter estimation. Thus, developing robust time-frequency analysis techniques to mitigate these effects is essential. Radar waveforms also often display nonstationary and transient behaviors due to factors like target dynamics or environmental conditions. Effective time-frequency distributions (TFDs) should capture these nonstationary aspects and accurately represent transient features. Efficient algorithms for real-time applications are also necessary to manage the computational complexity of TFDs. Balancing accuracy with computational efficiency is crucial for practical radar analysis. This paper explores the design and application of TFDs to address these challenges and improve radar system performance (Boashash, 2015; Ahmad *et al.*, 2019).

Corresponding author's e-mail address: aaashraf@nda.edu.ng

According to Kong et al. (2018), a method of recognizing low probability of intercept (LPI) waveforms that included polytime coded radar signals and robust performance comparison analysis was proposed. The method was based on CWD as the main TFD and CNN as the classifier. In addition to CWD and CNN, a sample averaging technique was also proposed to reduce the large computational cost required by intercept receivers in some situations. It was testified that the proposed technique offered significant improvement such as robustness to noise and recognition accuracy of 85% at SNR of -6 dB for all 12 signals. However, a large number of signal samples in thousands is required for good recognition accuracy as 22,680 and 9720 signals are required for training and validation respectively.

From Qu *et al.* (2018), the modulation of radar signals using the techniques of time-frequency analysis, image processing, and convolutional neural network (CNN) was identified. Through Cohen class time-frequency distribution (CTFD), the time-frequency images (TFIs) of received signals are extracted. To obtain the high-quality TFIs of received signals, a new kernel function for the CTFD was introduced, which has a stronger anti-noise ability than Choi–Williams time-frequency distribution. A series of image processing techniques, including 2-D Wiener filtering, bilinear interpolation, and the Otsu method, is applied to remove the background noise of the TFI and obtain a fixed-size binary image that contains only the morphological features of the TFI. We design a CNN classifier to identify the processed TFIs. The approach identifies up to 12 kinds of modulation signals, including frequency modulation, phase modulation, and composite modulation. Simulation results show that, for 12 kinds of modulation signals, an overall probability of successful recognition of 96.1% when SNR is −6 dB was achieved. However, the modulation recognition of the intra-pulse multi-component radar signal has become a problem to be solved.

According to Qu *et al.* (2019) a radar signal intra-pulse modulation recognition method based on convolutional denoising autoencoder (CDAE) and deep convolutional neural network (DCNN) was proposed. Cohen's TFD was used to convert radar signals into time-frequency images (TFIs). CDAE was designed to denoise and repair TFIs and a deep convolutional neural network based on Inception architecture was designed to identify the processed TFIs. The approach has good noise immunity and generalization. It can classify twelve kinds of modulation signals, and an overall probability of successful recognition is more than 95% when the SNR is -9 dB. A versatile method for different types of radar signals. However, the method developed has a very complicated classification structure and hence computationally complex.

A simple and effective FB algorithm based on Manhattan distance-based features (MDBFs) were proposed (Huang *et al.*, 2019). MDBFs are new features for radar signals that can be applied for the recognition of different modulations. The main contributions are First, radar signals are represented as wavelet ridges, which include important information that can distinguish different modulations, and the piecewise aggregate approximation algorithm is introduced to reduce signal dimensions. Then, the dynamic time warping averaging is employed instead of the traditional k-means algorithm to extract realistic centroids for each class. Finally, the Manhattan distances between each data sample and each centroid are used to construct MDBFs, and decisions are made using the k-nearest neighbor. It was proved that MDBFs have better class separability power than Euclidean-based features. MDBFs contain information about the correlations between different classes, which means that these features are suitable for

Corresponding author's e-mail address: aaashraf@nda.edu.ng

discriminating various modulations when their class distributions do not overlap badly in representation space. According to the parameter information, each modulation simulates twenty samples at SNR values of 10 to 15 dB to train the classifier. Each modulation generates one hundred samples at SNR values of [0, 3, 6, 9, 12] dB. Thus, a total of 900 samples are generated at each SNR to test performance. However, the proposed method is realized based on some known patterns, and future work will focus on applying the technique to an unknown modulated signal.

A rapid accurate recognition system, especially for when multiple signals arrive at the receiver was presented (Gao *et al.*, 2019). The system can recognize eight types of radar signals while separating signals: binary phase shift keying (BPSK), linear frequency modulation (LFM), Costas, Frank code, and P1–P4 codes. Regression variational mode decomposition (RVMD) is explored to separate the received signals, which saves time for parameter optimization of variational mode decomposition (VMD). The simulation results show that the recognition system achieves an overall recognition rate of 99.5% and 94% at a signal-to-noise ratio (SNR) of 0 dB when receiving single signals and double signals while spending 0.8 s and 2.23 s, respectively. Furthermore, the proposed system can also be used to recognize mechanical and medical signals. However, further related research will be required to examine the ideal technology required for an unknown number of radar signal recognitions in a more realistic environment.

The usefulness of an algorithm in the scenario of LPI radar signal detection and recognition based on visibility graphs (VG) was explored (Tao *et al.*, 2020). More network and feature information can be extracted in the VG two-dimensional space, this algorithm can solve the problem of signal recognition using the autocorrelation function. Signal detection simulation analysis shows that when the SNR is −10 dB, the SDP is 90.9%, and as the SNR increases, the SDP also increases, especially when SNR is greater than −8 dB, the SDP is 100%. However, future research was expected to extend the VG theory to radar signal sorting and working pattern recognition applications.

A novel intra-pulse modulation recognition method based on the high-order spectrums of radar signals was developed (Chen *et al.*, 2021). Automatic soft thresholding is implemented in the deep residual network to adaptively eliminate redundant information in the process of feature learning and improve the learning effect of valuable features in distribution images of corresponding third-order spectrums. The extensive simulations compared with the other four methods further reveal the excellent classification performance of the proposed method. The approach achieves an overall probability of successful recognition of 93.5% for eight kinds of modulation signals, even when the SNR is just − 8 dB. Outstanding performance proves the superiority and robustness of the proposed method. However, it has recognition mistakes that mainly occur between the signal pairs that have similar TSDIs, such as EQFM and Frank code signals, LFM and Frank code signals, and the process of image resizing also makes small frequency jump blurred. The losses and blurs of this small frequency information finally led to confusion between signals.

According to Matuszewski and Pietrow (2021), recognition method of emitted radar signals with agile waveforms based on the convolutional neural network (CNN) was presented. These signals are measured in the electronic recognition receivers and processed into digital data, after which they undergo recognition. The implementation of this system is presented in a

Corresponding author's e-mail address: aaashraf@nda.edu.ng

simulation environment with the help of a signal generator that can make changes in signal signatures earlier recognized and written in the emitter database. The effectiveness results of the applied solutions and the possibilities of developing the method of learning and processing algorithms are presented utilizing tables and appropriate figures. The experimental results demonstrate that the proposed method can effectively solve the problem of recognizing raw radar signals with agile time waveforms and achieve correct probability of recognition at the level of 92–99%. However, the size of the CNN use cannot be used in the case of direct operation at high frequencies.

Therefore, this paper in line with the reviewed research focused on normal radar signal analysis (of lesser attention, yet still important) using different time-frequency distributions.

2. Material and Method

The radar signal is modeled based on the pulse-to-pulse constant frequency, pulse width (PW), and pulse repetition period (PRP); hence, its name is normal radar signal due to this constancy. Fast Fourier transform was used for the frequency representations and conversion process. However, the fast Fourier transform produced mirrored frequencies that resembled the actual signal but appeared at different frequencies which are not required. As such, the Hilbert transform was used to help in eliminating the mirrored signal that was caused by the fast Fourier transform. And finally, the signal was analyzed using the TFDs considered in this work. The normal signal model is based on equation (1) (Wiley, 2006):

$$s(t) = Asin(2\pi f\tau) \tag{1}$$

where A is amplitude in pu, f is the center/modulating frequency in Hz, τ is the PW in secs; duration of the signal in which the signal is On. The Off time (called the listening time) is simply modelled by zeroes for the considered duration. A full complete radar signal cycle concatenation of the On and Off times (Wiley, 2006; Ahmad *et al.*, 2023). The time-frequency analysis tools proposed for this paper include WVD, WWVD, FWVD, CWD, and hybrid distributions that combined FWVD and CWD. Further information on these TFDs is given in the preceding subsections.

2.1 Wigner-Ville Distribution (WVD)

WVD is an important quadratic time-frequency distribution (QTFD) that extends the capabilities of the Wigner distribution. It employs a quadratic function to achieve precise localization for linearly modulated frequency and impulse signals. the WVD equation is also divided into two major sections (Ahmad *et al.*, 2019). The first stage is for obtaining instantaneous autocorrelation function (IAF) (2) and the second stage is the time-frequency conversion and storage of the IAF based on the Fourier transform (3):

$$K_z(t,\tau) = z\left(t+\frac{\tau}{2}\right)z^*\left(t-\frac{\tau}{2}\right) \tag{2}$$

$$\rho_{z,WVD}(t,f) = \int_{-\infty}^{\infty} K_z(t,\tau)e^{-j2\pi f\tau}d\tau \tag{3}$$

Where $\rho_{z,WVD}(t,f)$ represents the Wigner-Ville distribution of a signal at time t and frequency f. $z\left(t+\frac{\tau}{2}\right)$ represents a complex-valued function, typically denoting the analysing signal or

Corresponding author's e-mail address: aaashraf@nda.edu.ng

window function used in the WVD. $*$ (superscript) represents the complex conjugate. The interference terms are independent of the time-frequency distance between the two signal terms. In some applications, they may overlap the auto-components (Boashash, 2015). Moreover, since (3) requires an evaluation from minus infinity to plus infinity, which is impossible in the real application, pseudo-Wigner-Ville distributions (PWVDs) are chosen to use a running window to overcome this problem (Boashash, 2015). Putting a regular window into (3) leads to PWVD (Stephens, 1996):

$$\rho_{z,PWVD}(t,f) = \int_{-\infty}^{\infty} h(\tau) z\left(t+\frac{\tau}{2}\right) z^*\left(t-\frac{\tau}{2}\right) e^{-j2\pi f\tau} d\tau \quad (4)$$

For this research, the two basic forms of pseudo-WVD were considered, which are windowed WVD (WWVD) and filtered WVD (FWVD).

2.2 Windowed Wigner -Ville Distribution (WWVD)

Similar to the WVD, the WWVD follows a comparable process. However, an additional step is introduced before the conversion, involving the application of a windowing technique to the instantaneous autocorrelation function (IAF) to enhance its smoothness. For this purpose, a Hamming window is chosen due to its desirable characteristics, including a relatively narrow main lobe width and effective attenuation of the initial side lobes (Cheng *et al.*, 2022). Equation (5) illustrates the windowing process applied to the instantaneous autocorrelation function (IAF), while equation (6) represents the final equation of the Wigner-Ville distribution (WVD) incorporating this windowing process and equation (7) represents the hamming window used.

$$K_{z,w}(t,\tau) = g_w(\tau) K_z(t,\tau) \quad (5)$$

$$\rho_{z,WWVD}(t,f) = \int_{-\infty}^{\infty} g_w(\tau)\, z\left(t+\frac{\tau}{2}\right) z^*\left(t-\frac{\tau}{2}\right) e^{-j2\pi f\tau} d\tau \quad (6)$$

$$\rho_{z,WWVD}(t,f) = \int_{-\infty}^{\infty} 0.54 - 0.46\cos\left(\frac{2\pi\tau}{T}\right)\ z\left(t+\frac{\tau}{2}\right) z^*\left(t-\frac{\tau}{2}\right) e^{-j2\pi f\tau} d\tau \quad (7)$$

Where $\rho_{z,WWVD}(t,f)$ represents the windowed Wigner-Ville distribution of a signal at time t and frequency f.$z\left(t+\frac{\tau}{2}\right)$ represents a complex-valued function, typically denoting the analyzing signal or window function used in the WVD. $*$ represents the complex conjugate.

2.3 Filtered Wigner-Ville Distribution (FWVD)

The FWVD follows a similar approach to the WWVD. However, instead of applying a windowing technique, a filtering process, which can be considered a convolution process, is employed. Equation (8) represents the filter Wigner-Ville distribution, which encapsulates this filtering process. To accomplish the filtering, the Kaiser window is utilized due to its effectiveness in suppressing unwanted noise or interference while preserving the desired signal components in radar signals. The Kaiser window's parameter, referred to as the beta value, allows for fine-tuning the balance between the width of the main lobe and the levels of the sidelobes. By adjusting the beta value, engineers can effectively reduce the sidelobes and improve the selectivity of the filtering process, thereby enhancing the overall performance of the radar system (Liang *et al.*, 2021).

$$K_{z,f}(t,\tau) = g_f(t) {}^{*}_{t} K_z(t,\tau) \quad (8)$$

Corresponding author's e-mail address: aaashraf@nda.edu.ng

$$\rho_{z,FWVD}(t,f) = \int_{-\infty}^{\infty} g_f(t) * z\left(t+\frac{\tau}{2}\right) z^*\left(t-\frac{\tau}{2}\right) e^{-j2\pi f\tau} d\tau \quad (9)$$

$$\rho_{z,FWVD}(t,f) = \int_{-\infty}^{\infty}\int_{-\infty}^{\infty} \frac{I_0\left\{\beta\sqrt{1-\left(\frac{t-u}{T}\right)^2}\right\}}{I_0\{\beta\}} z\left(u+\frac{\tau}{2}\right) z^*\left(u-\frac{\tau}{2}\right) e^{-j2\pi f\tau} du d\tau \quad (10)$$

$\rho_{z,FWVD}(t,f)$ represents the pseudo-filtering, $\frac{I_0\left\{\beta\sqrt{1-\left(\frac{t-u}{T}\right)^2}\right\}}{I_0\{\beta\}}$ represents the filtering process added to equation (4).

2.4 *Choi-Williams Distribution (CWD)*

The CWD belongs to the Cohen class of time-frequency distributions. It incorporates a kernel function that effectively suppresses cross-terms resulting from multiple signals. Consequently, the CWD exhibits high resolution and minimizes the presence of cross terms (Guo, Yu, & Ruan, 2019). This TFD, unlike WVD, is readily available and there was no need for its pseudo-version design therefore it was adopted from the standard reference (Boashash, 2015). Mathematically, the expression for the CWD can be represented as follows:

$$\rho_{z,CWD}(t,v) = 2\iint_{-\infty}^{+\infty} \frac{\sqrt{\sigma}}{4\sqrt{\pi}|\tau|} e^{-v^2\sigma/(16\tau^2)} z\left(t+v-\frac{\tau}{2}\right) z^*\left(t+v-\frac{\tau}{2}\right) e^{-j2\pi v\tau} dv d\tau \quad (11)$$

Where t and f represent time and frequency, $e^{\frac{-\pi^2\sigma(t-u)^2}{\tau^2}}$ It represents a Gaussian function in the time domain function, σ is the positive scaling factor, $e^{-j2\pi f\tau}$ it represents a complex exponential function in the frequency domain and $dud\tau$ it represents the integration variables. However, this adopted version was modified using two smoothing for both time and frequency to get its pseudo version.

2.5 *Hybrid TFD*

The hybrid TFD in this research was constructed by combining two TFDs, namely the FWVD and the CWD. Among the various WVDs considered in this paper, FWVD was chosen as the representative due to its superior ability to suppress cross-terms and frequency cross-talk, resulting in the best performance. Mathematically, the hybrid TFD can be expressed in equation (12) as follows:

$$\rho_{z,hybrid}(t,v,f) = \int_{-\infty}^{\infty}\int_{-\infty}^{\infty}\int_{-\infty}^{\infty} \frac{\sqrt{\sigma}}{2\sqrt{\pi}|\tau|} \frac{I_0\left\{\beta\sqrt{1-\left(\frac{t-u}{T}\right)^2}\right\}}{I_0\{\beta\}} e^{-v^2\sigma/(16\tau^2)} z\left(u+v-\frac{\tau}{2}\right) z^*\left(u+v-\frac{\tau}{2}\right) e^{-j2\pi f v\tau} du dv d\tau \quad (12)$$

It is seen from equation (12) that the hybrid version is a filtered version of the doubled windowed CWD, hence an extra integration is added to cater for the filtering process, and also the time parameter is changed to the convolution parameter. Furthermore, careful observation of equation (11) shows that the CWD can be considered a pseudo-WVD. That uses an exponential function (hence, sometimes called exponential distribution) (Boashash, 2015). As such, only the Kaiser filtering window was integrated into the CWD as the CWD already contains the IAF of WVD. However, the result obtained showed no noticeable difference from that obtained from CWD. As such, a second hybrid was developed by simply multiplying the output of FWVD and that of CWD

Corresponding author's e-mail address: aaashraf@nda.edu.ng

3. Results and Discussion

Graphical Interpretation of the Analysis Based on TFDs:

A waterfall presentation of the analysis based on TFDs such as WVD, WWVD, FWVD, CWD, and hybrid distributions that combined FWVD and CWD involves a 3D plot with the x-axis representing time, the y-axis representing frequency, and the z-axis representing power. In this presentation, the x-axis is labeled as time and represents the progression of time throughout the analyzed signal. The y-axis is labeled as frequency and represents the range of frequencies under examination. The z-axis is labeled as power, which indicates the magnitude or strength of the signal at each specific time-frequency point. The waterfall presentation provides a visual representation of how the signal's spectral content changes over time. Each point on the plot corresponds to a specific time-frequency location, and the color or intensity at that point represents the power or magnitude of the signal. By observing the waterfall presentation, analysts can gain insights into the time-varying behavior of the signal's frequency components. They can identify frequency trends, variations, and patterns that occur over different time intervals. The z-axis, representing power, allows analysts to assess the strength or energy distribution of the signal at various time-frequency points. In summary, a waterfall presentation based on WVD, WWVD, FWVD, CWD, and hybrid distributions combines the elements of time, frequency, and power to visually depict the signal's changing spectral content over time. This presentation facilitates the analysis of temporal frequency patterns and the power distribution of the signal at different time-frequency locations.

3.1 Waterfall Presentation of NWVD

Figure 1 shows a three-dimensional (3D) result obtained for a normal radar signal using NWVD.

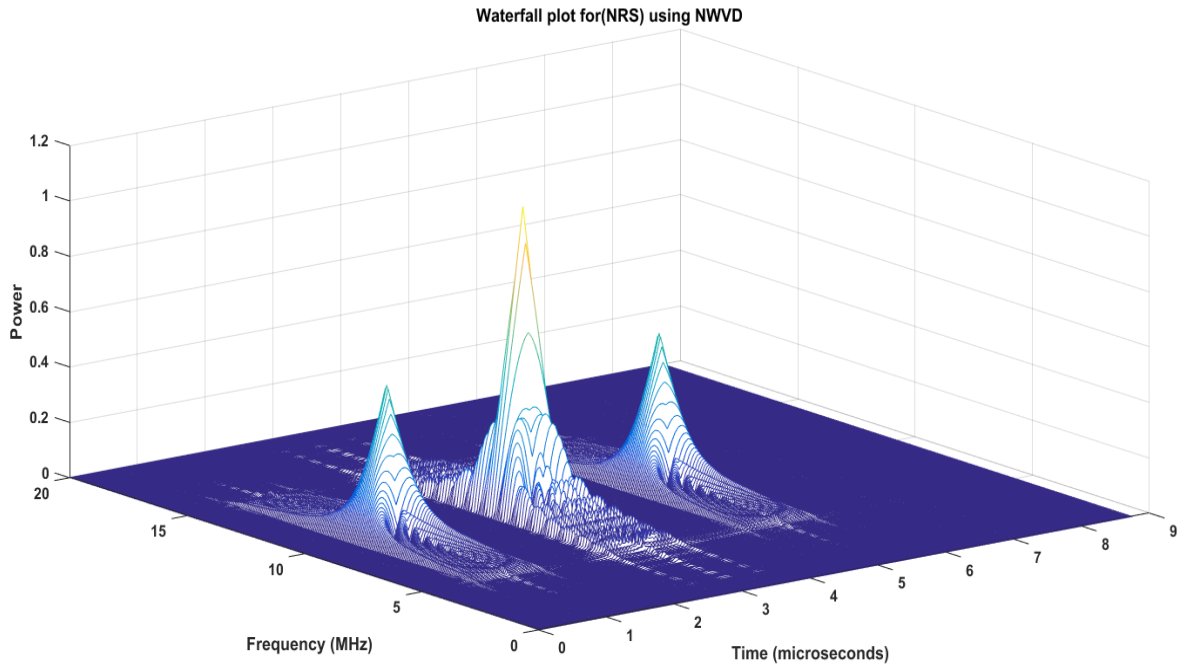

Figure 1: waterfall 3-D presentation of NRS using NWVD

Figure 1 shows a three-dimensional (3D) waterfall plot of power, time, and frequency for the normal radar signal using NWVD. The signal was generated at a center frequency of 10 MHz which indicates that the radar system operates around this frequency, sampling frequency of

40 MHz indicates that the signal was digitized at a rate of 40 million samples per second, capturing detailed information about the signal, Pulse width (PW) of 1 μs which refers to the duration of each transmitted radar pulse. A shorter pulse width allows for better range resolution in radar systems, Pulse Repetition Interval (PRI) or pulse repetition time (PRT) of 2μs indicates the time interval between consecutive pulses. This parameter determines the radar's maximum unambiguous range and affects the radar's ability to distinguish between different targets and a delay of a quarter at the beginning of the pulse suggests that there is a time delay introduced at the start of each pulse, corresponding to a quarter of the pulse width. This delay is often used to separate the transmitted pulse from any reflections or clutter that may be present in the radar system based on reviewed literature of chapter two. The essence of showing the 3D plot is for the analysts to gain insights into the radar signal's time-varying spectral content. Observing how the signal's power is distributed across different frequencies at different time points, allows for the identification of frequency components, temporal patterns, and potential targets or objects in the radar's field of view. However, it can be seen from the plot between the 2 pulses there is a cross-terms that resemble the signal but not the actual signal it occurs due to the interaction of the main signal with the noise. Thereafter, the Hilbert transform was used in the process to eliminate the negative mirrored signal since the focus of the project is on the main signal.

3.2 Waterfall Presentation of WWVD

Figure 2 shows a 3D result obtained for a normal radar signal using WWVD.

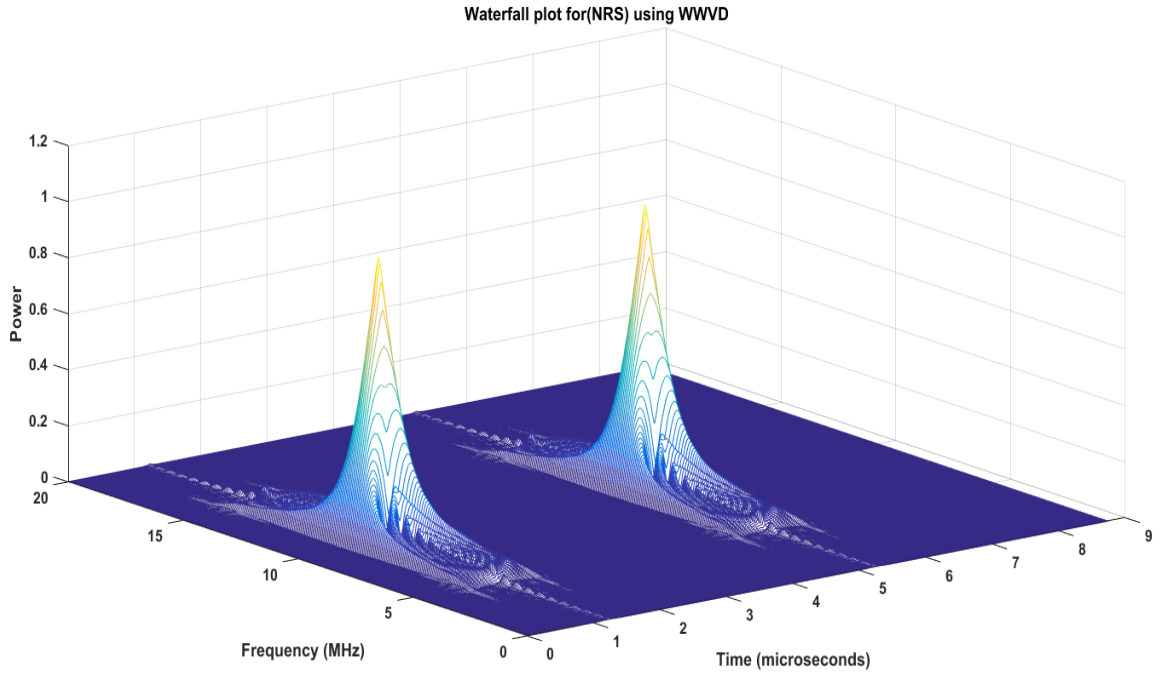

Figure 2: waterfall 3-D presentation of NRS using WWVD

Figure 2 shows a 3D waterfall plot of power, time, and frequency for the normal radar signal using WWVD. Based on the information that was presented in the methodology, the signal was generated with the same characteristics as that of NWVD. However, from the result obtained for these waterfalls of WWVD, the cross-term was completely eliminated due to the effect of the windowing.

3.3 Waterfall Presentation of FWVD

Figure 3 shows a 3D result obtained for a normal radar signal using FWVD.

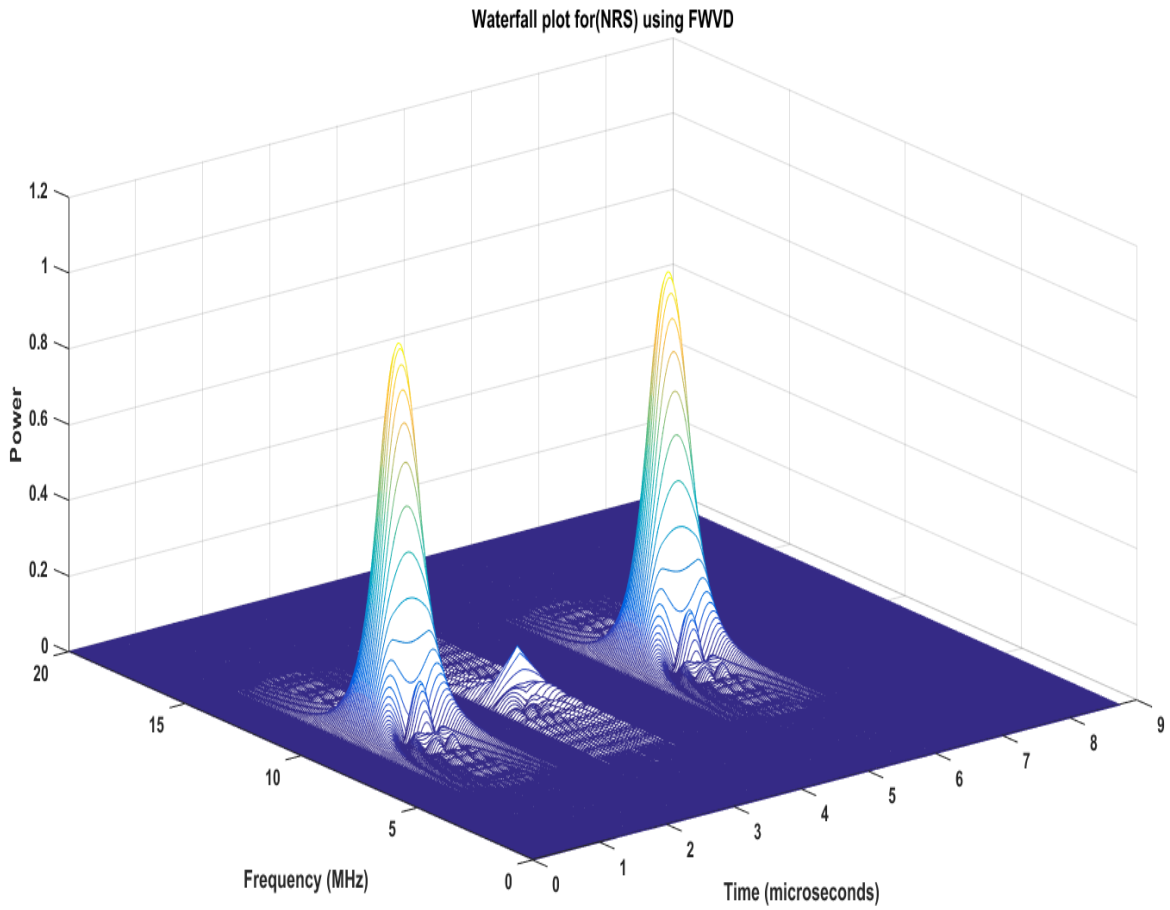

Figure 3: waterfall 3-D presentation of NRS using FWVD

Figure 3 shows a 3D waterfall plot of power, time, and frequency for the normal radar signal using FWVD. Based on the information that was presented in the methodology, the signal was generated with the same characteristics as that of NWVD. From the pictorial view, it was observed that the effect of cross terms was little compared to that of NWVD. However, the reduction of the cross terms was due to the filtering process of the FWVD.

Corresponding author's e-mail address: aaashraf@nda.edu.ng

3.4 Waterfall Presentation of CWD

Figure 4 shows a 3D result obtained for a normal radar signal using CWD.

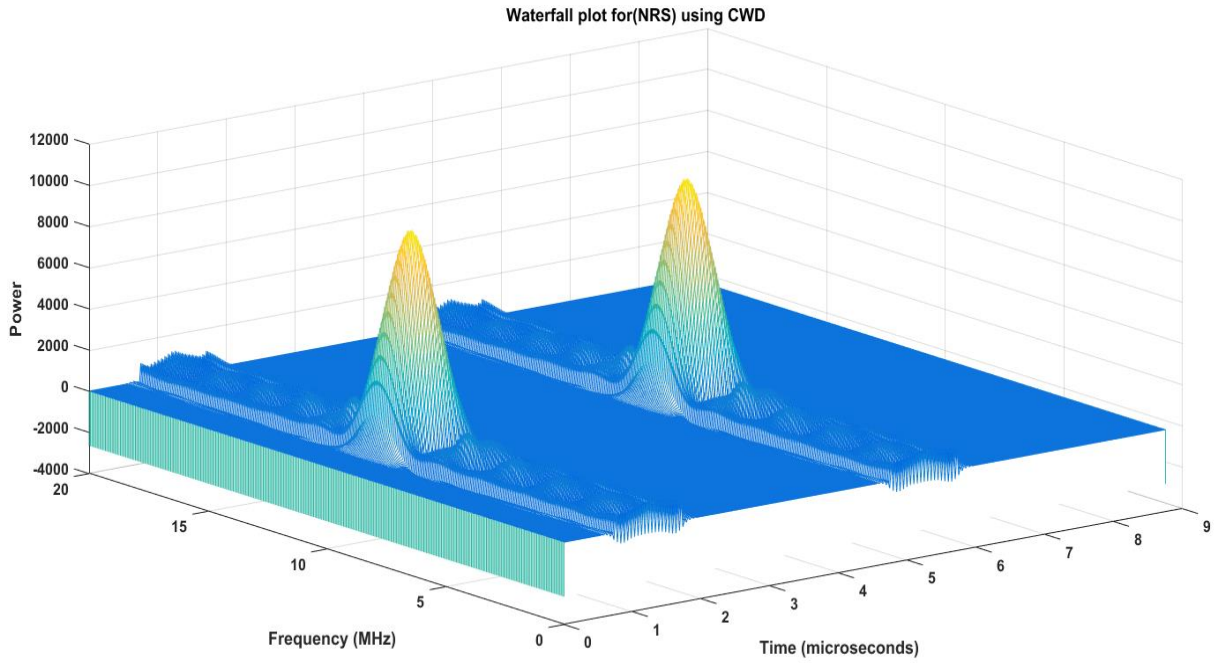

Figure 4: waterfall 3-D presentation of NRS using CWD

Figure 4 shows a 3D waterfall plot of power, time, and frequency for the normal radar signal using CWD. Based on the information that was presented in the methodology, the signal was generated with the same characteristics as that of NWVD. The pictorial view of the CWD shows that the signal is well captured with no cross-terms or inner artifact.

3.5 Waterfall Presentation of HYBRID (FWVD & CWD)

Figure 5 shows a 3D result obtained for a normal radar signal using a hybrid.

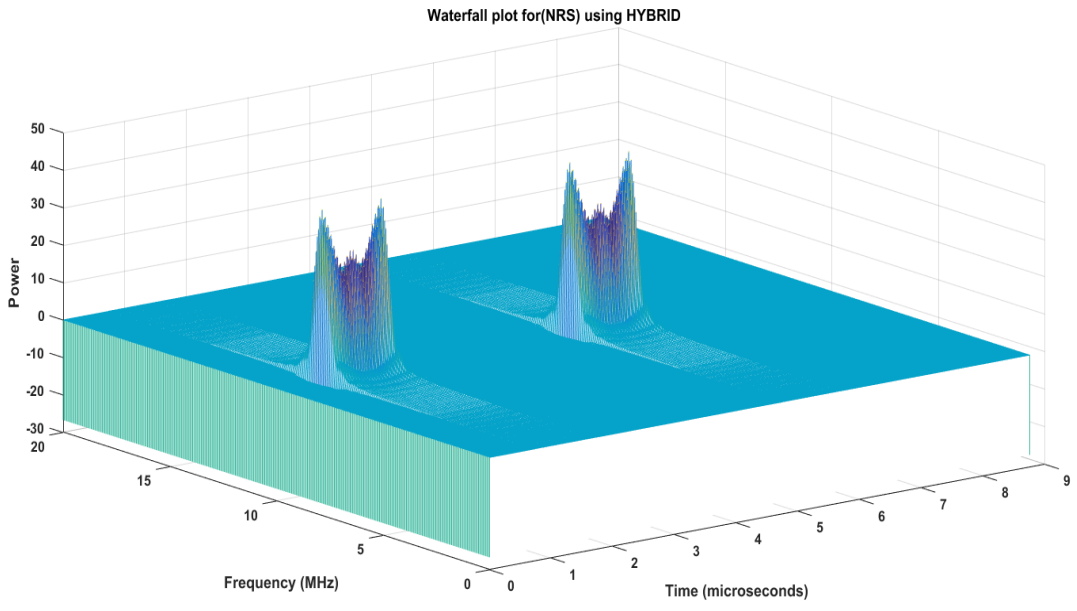

Figure 5: waterfall 3-D presentation of NRS using Hybrid (FWVD &CWD)

Corresponding author's e-mail address: aaashraf@nda.edu.ng

Figure 5 shows a 3D waterfall plot of power, time, and frequency for the normal radar signal using a hybrid. Based on the information that was presented in the methodology, the signal was generated with the same characteristics as that of NWVD. The pictorial view of the hybrid shows how the signal was well captured with no cross-terms or inner artifact. However, the shape of the captured signal using this hybrid shows a pre-indication that further analysis such instantaneous power or frequency may not yield accurate results when compared to others. Generally, all the TFDs considered for analysis in this research accurately captures the time and frequency changes of the normal radar signal graphically to a high degree. Exact numerical accuracy would depend on further analysis using feature extraction and classification for future works.

5. Conclusion

The paper conducted analysis of normal radar signals, exploring various time-frequency distribution configurations, including WVD, WWVD, FWVD, CWD, and a hybrid distribution that combines FWVD and CWD. The research revealed that most of these time-frequency distributions (TFDs) effectively captured the time and frequency characteristics of radar signals, which were modeled based on specific pulse width (PW), pulse repetition interval (PRI), center frequency, and sampling frequency. The values of these parameters are PWof 1µs, PRIof 2µs, center frequency of 10 MHz, and sampling frequency of 40 MHz. As a result of these findings, it is evident that these TFDs hold great potential for further analysis of other radar signal types using signal processing and classification tools. Instantaneous power, instantaneous frequency, and machine learning techniques can also be employed for automatic waveform recognition. This advancement could significantly enhance radar signal processing capabilities and contribute to improved radar system performance and accuracy.

Reference

Ahmad, AA., Aji, MM., Abdulmumin, Y., Jae, IA. and Bello-Imokhuede, UI. 2023. Profiling radar signals based on pulse-to-pulse frequency agility. Global Journal of Engineering and Technology Advances, 15(2): 141–149.

Ahmad, AA., Ajiya, M., Yusuf, ZY. and Airoboman, AE. 2019. On the identification of low probability of intercept radar signals using time-frequency signal analysis and processing. Journal of Electrical and Electronics Engineering, 12(2): 5–10.

Boashash, B. 2015. Time-frequency signal analysis and processing: A comprehensive reference (2nd ed.,). Academic Press, Massachusetts, USA., pp. 3-56.

Chen, K., Zhu, L., Chen, S., Zhang, S. and Zhao, H. 2021. Deep residual learning in modulation recognition of radar signals using higher-order spectral distribution. Measurement, 185: 109945 (1-12).

Cheng, J., Li, J., Zhang, R., Liu, F., Chen, X., Zhao, Z., Zhan, Y. and Kazemzadeh, S. 2022. Based on FPGA laser spectrum analysis system. In Proceedings of the 2nd International Conference on Cognitive Based Information Processing and Applications (CIPA 2022), Changzhou, China, 2–3 September 2022., 2: 81–89.

Gao, J., Shen, L., Gao, L. and Lu, Y. 2019. A rapid accurate recognition system for radar emitter signals. Electronics, 8(4): 463 (1-14).

Corresponding author's e-mail address: aaashraf@nda.edu.ng

Guo, Q., Yu, X. and Ruan, G. 2019. LPI radar waveform recognition based on deep convolutional neural network transfer learning. Symmetry, 11(4): 540 (1-17).

Gulum, TO. 2007. Autonomous non-linear classification of LPI radar signal modulations Doctoral dissertation, Naval Postgraduate School, Monterey, California.

Huang, Y., Jin, W., Li, B., Ge, P. and Wu, Y. 2019. Automatic modulation recognition of radar signals based on Manhattan distance-based features. IEEE Access, 7: 41193–41204.

Kong, S.-H., Kim, M., Hoang, LM. and Kim, E. 2018. Automatic LPI radar waveform recognition using CNN. IEEE Access, 6: 4207–4219.

Liang, C., Teng, Z., Li, J., Yao, W., Hu, S., Yang, Y. and He, Q. 2021. A Kaiser window-based S-transform for time-frequency analysis of power quality signals. IEEE Transactions on Industrial Informatics, 18(2): 965–975.

Matuszewski, J. and Pietrow, D. 2021. Specific radar recognition based on characteristics of emitted radio waveforms using convolutional neural networks. Sensors, 21(24): 8237 (1-19).

Pace, PE. 2009. Detecting and classifying low probability of intercept radar. Artech House, Norwood, USA., pp. 4-65.

Patole, SM., Torlak, M., Wang, D. and Ali, M. 2017. Automotive radars: A review of signal processing techniques. IEEE Signal Processing Magazine, 34(2): 22–35.

Qu, Z., Mao, X. and Deng, Z. 2018. Radar signal intra-pulse modulation recognition based on convolutional neural network. IEEE Access, 6: 43874–43884.

Qu, Z., Wang, W., Hou, C. and Hou, C. 2019. Radar signal intra-pulse modulation recognition based on convolutional denoising autoencoder and deep convolutional neural network. IEEE Access, 7: 112339–112347.

Stephens, JP. 1996. Advances in signal processing technology for electronic warfare. IEEE Aerospace and Electronic Systems Magazine, 11(11): 31–38.

Tao, WAN., Kaili, J., Jingyi, L., Yanli, T. and Bin, T. 2020. Detection and recognition of LPI radar signals using visibility graphs. Journal of Systems Engineering and Electronics, 31(6): 1186–1192.

Upperman, TL. 2008. ELINT signal processing using Choi-Williams distribution on reconfigurable computers for detection and classification of LPI emitters. Doctoral dissertation, Naval Postgraduate School, Monterey, California.

Ünal, L. and Pakfiliz, AG. 2022. LPI radar signal detection based on autocorrelation function and Wigner-Ville distribution. Revista de Ingeniería de Computación, 9(4): 53-62.

Wei, P., Sili, L. and Hongzhi, D. 2014. The application of adaptive genetic algorithms in single-resistant radar jamming. In The 26th Chinese Control and Decision Conference (2014 CCDC), Changsha, China, 31 May–2 June 2014. 1322-1327.

Corresponding author's e-mail address: aaashraf@nda.edu.ng

Wiley, R. 2006. ELINT: The interception and analysis of radar signals. Artech House, Massachusetts, USA. 8-26

Corresponding author's e-mail address: aaashraf@nda.edu.ng